Original Research Paper

Experimental Evaluation of Adaptive Step-Size Based FxLMS Approach for Active Noise Control in Magnetic Resonance Imaging Systems

[1]I. Juvanna, [2]Uppu Ramachandraiah, [2]G. Muthukumaran, [2]Kawin Subramaniyam and [2]G. Nethra

[1]Department of Information Technology, Hindustan Institute of Technology and Science, India
[2]Centre for Sensors and Process Control, Hindustan Institute of Technology and Science, India

Abstract: Magnetic Resonance Imaging (MRI) scanners emit up to 135 decibels of acoustic noise, which is a major source of discomfort for patients and personnel evaluating them during routine medical scans, necessitating the development of a method to reduce the acoustic noise generated during MRI testing. The goal of this study is to propose a frequency-domain Active Noise Control (ANC) method for acoustic noise reduction in MRI and to demonstrate its ANC effectiveness on an experimental MRI scanner model specifically built for this purpose. In comparison to the standard Least Mean Square (LMS) algorithm, we used the Filtered-x Least Mean Square (FxLMS) approach with an adaptive variable step-size approach to adjust the filter coefficients dynamically, which considerably enhances the ANC system's convergence and reduces acoustic noise. The simulation results obtained from the MATLAB Simulink model on a pre-recorded 30-sec MRI noise signal represented by the step-size variation over time, error and noise convergence plots reveal that the adaptive step-size FxLMS (ASFxLMS) technique increases noise and error convergence rate significantly more than existing ANC algorithms to facilitate its use during MRI scans. Experimental results with our functional MRI (fMRI) testbed show approximately 25-dB overall noise reduction relative to the noise levels without ANC.

Keywords: Active Noise Cancellation, Adaptive Step-Size Filtered-x Least Mean Square, Magnetic Resonance Imaging, MATLAB Simulink

Introduction

MRI is a highly sophisticated medical screening tool that has become an invaluable asset to modern medicine due to its ability to conduct in-depth and non-invasive studies of the human body (Takkar *et al.*, 2017). Regrettably, the loud noise generated during scanning is uncomfortable, may be detrimental to patients, and may hinder imaging protocol. Specifically, high-intensity acoustic noise may induce anxiousness and the small-bore diameter of scanners may present difficulties for claustrophobic people. This has spiked tremendous interest in enhancing patient comfort during MRI tests (Siddiqui *et al.*, 2017).

Due to the interaction of the electrical current passing through the gradient coils in the presence of a static magnetic field, Lorentz forces are generated. As the current changes polarity, these forces cause the MRI-supporting structure to rapidly change dynamic stresses and deformation. The structure's resulting vibration makes it act like a loudspeaker, thus emitting a high level of noise into the air (Roozen *et al.*, 2008). The resultant Sound Pressure Level (SPL) is proportional to the strength of the magnetic field and the parameters involved. On MRI with a magnetic field greater than 3T, sound pressure levels greater than 130 dB have been measured (Price *et al.*, 2001).

Previously, several different approaches to noise reduction, in general, have been implemented with modest effectiveness. Controlling the noise level which is generated by the MRI has resulted in an ocean of research aimed at characterizing acoustic noise. The classical passive approaches to noise reduction involve using passive earplugs for sealing off the noise, sequence optimization, antiphase noise, and redesigning and retrofitting gradient coil hardware (McJury, 2021). The use of earphones in patients undergoing general anesthesia during MRI considerably minimizes involuntary arm and leg movement. Acute changes in hearing thresholds have been observed in individuals who

were scanned without wearing ear protection. Thus, reducing acoustic noise signals during MRI can improve patient comfort and the acceptability of the technique. However, these attenuate signals across a wide frequency range but underperform when applied to low-frequency frequencies (Facciolo *et al.*, 2017).

While passive noise control is based on the absorption of noise signals, ANC is based on a fundamentally different technique. ANC is founded on an electroacoustic technology that negates the primary noise using the superposition principle (Kuo *et al.*, 2003). To superimpose and cancel out this noise signal, a signal identical in size but out-of-phase with the noise signal is generated. Given the fact that the properties of the noise source and the path it takes vary over time, an adaptive control mechanism is required to minimize MRI noise. The coefficients of the filters employed in these systems are adjusted to reduce the error signal. When higher wavelength signals are present, the active way of noise cancellation is more productive than the passive approach (Lin *et al.*, 2005).

ANC has been used to MRI noise earlier (Chambers *et al.*, 2007), with observed noise reductions of roughly 15 to 25 dB. These investigations, however, have the following limitations. To begin with, noise reduction tests were conducted using computer models or in a laboratory setting, rather than in actual MRI rooms. Also, all trials used a headphone system, which precluded vocal communication between medical professionals and the patient providing a feeling of anxiety and isolation in the external auditory environment. Third, none of the research evaluated the user's motions. As a result, the findings of these investigations were of limited utility to medical personnel (Rudd *et al.*, 2012).

ANC controllers can be generically classified as feedback or feedforward. When the filter has access to reference noise and the noise associated with this noise needs to be reduced, feedforward control is used as represented in Fig. 1 (Wu *et al.*, 2014). The error signal is used to update the adaptive filter's weights. A feedforward system might well be narrowband or broadband in nature. On the other hand, a feedback control system simply uses one error sensor to provide negative feedback and adjusts the weights on the filter accordingly (Kuo *et al.*, 2006). However, we can also adopt a hybrid technique whose advantage lies in its ability to enable the use of a lower-order filter to attain the same performance as the above two methods.

Numerous approaches can be used to implement ANC filter blocks; Transversal adaptive ANC that makes use of an adaptive filter, Finite Impulse Response (FIR), or Infinite Impulse Response (IIR) realizations; Frequency domain ANC is the fastest since it transfers all signals to the frequency domain utilizing Fast Fourier Transform (FFT) before doing computations. Sub-band ANC is utilized in the case of long tap lengths and for the

processing of sub-band signals, resulting in a decreased computational load and faster convergence; Modal ANC, which breaks down the ANC problem, hence lowering computation and increasing convergence, as well as ANC based on Recursive Least Squares (RLS), among others (Lu *et al.*, 2021; Panda and Puhan, 2016).

The devices used to implement ANC, such as digital filters, anti-aliasing filters, Analog-to-Digital Converters (ADC), and Digital-to-Analog Converters (DAC), contribute to noise as well (Khan *et al.*, 2012). This creates a secondary path, which must be estimated to produce a correct anti-noise signal. The exact estimation of this channel improves the effectiveness of ANC. There are two primary strategies for compensating for this secondary route. One method is to connect an inverse filter, *1/S(z)*, to the secondary path *S(z)*. The second method (Chang *et al.*, 2018) is to include an identical filter $S(z)$ in the reference signal path of the LMS algorithm's weight update, which actualizes the FxLMS algorithm as represented in Fig. 2.

In the functional domain of the acoustic chamber, the conventional FxLMS approach is formulated to reduce the specific acoustic modes. The modal FxLMS approach obtained *x(n)* by processing the reference signal by modal secondary channels as opposed to physical secondary routes. This reduces the signal by modal secondary channels as opposed to physical secondary routes. This reduces the computational cost of filtering the *x(n)* with *S(z)*, as well as the acoustic potential energy required for overall noise reduction. Many variants of FxLMS have been created by tweaking the original FxLMS approach (Mazur *et al.*, 2018).

A fixed step size is employed in the FxLMS method, which enables ANC systems to achieve an acceptable convergence speed in stationary noise situations, though at a slower rate than the filtered-x recursive least squares (FxRLS) technique. To obtain a fast-converging algorithm in both stationary and nonstationary situations, it may be worthwhile to experiment with a variable step size in the FxLMS algorithm. If properly developed, an adaptive threshold FxLMS algorithm would convergent as rapidly as the FxLMS algorithm and monitor the stochastic noise environment faster than both FxLMS and FxRLS, at the expense of a minor increase in processing cost (Zeb *et al.*, 2017).

Signal processing applications have adopted the concept of using various step sizes or user parameters to control the rate of convergence of LMS-like algorithms. For ANC, researchers have tailored its use for online secondary-path modeling (Akhtar *et al.*, 2007), online feedback-path modeling (Haseeb *et al.*, 2018), and FIR controllers (Akhtar and Mitsuhashi, 2011).

Continuous advances in the fields of Digital Signal Processing (DSP) have created an opportunity to adopt ANC to reduce MRI noise using highly advanced algorithms that are more dependable and resilient in

suppressing noise in real-time. This research aims to measure the performance of an acoustic noise cancellation system based on adaptive variable step-size FxLMS for noise reduction in MRI scanners. A noise processing pipeline was constructed and analyzed using the MATLAB Simulink (Math Works, USA) framework, which enables an in-depth examination of key elements of MRI noise characteristics, including noise, error, and convergence. To summarize, the existing approaches use optical microphones for sensing very expensive sound, and modifying the pulse sequences is a complicated process that needs expertise, hence without any modification of existing machine hardware and pulse sequence, with the help of a very Simple Micro-Electromechanical System (MEMS) microphones and tiny speakers (with less cost) we can achieve the noise reduction which is the salient feature of this research.

Our contributions to the work include:

- We propose a novel ASF LMS algorithm that incorporates both residual noise and an adaptive variable step-size approach that adjusts automatically to minimize error rates
- Achieve faster convergence in reducing the noise decibels and error rate
- The results achieved through the simulation validate the improved performance of our approach in MRI acoustic noise reduction
- The conducted experiment also asserts the superiority of our method in reducing the MRI noise reflected in the comparison of the results with ANC ON/OFF
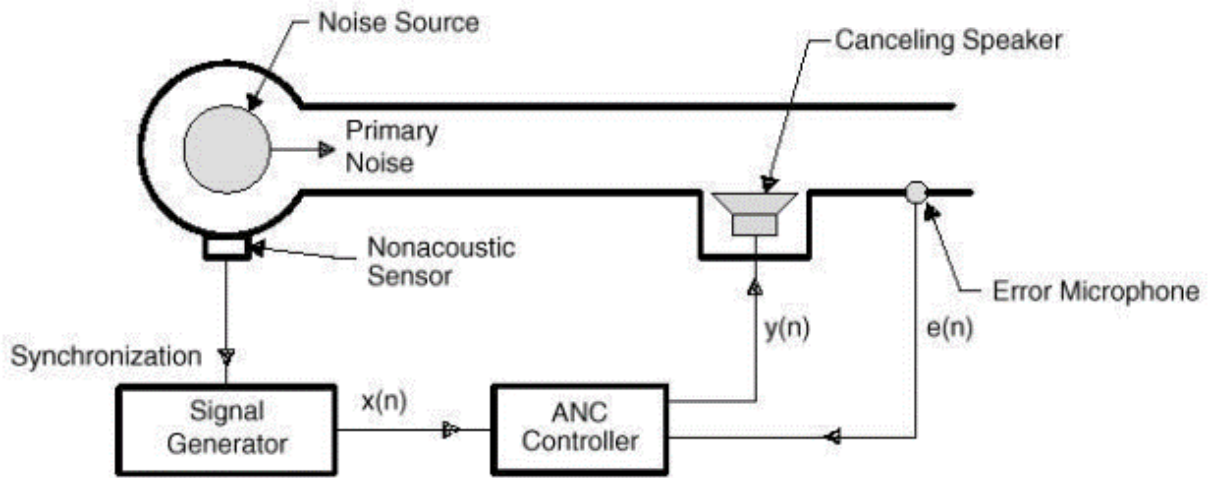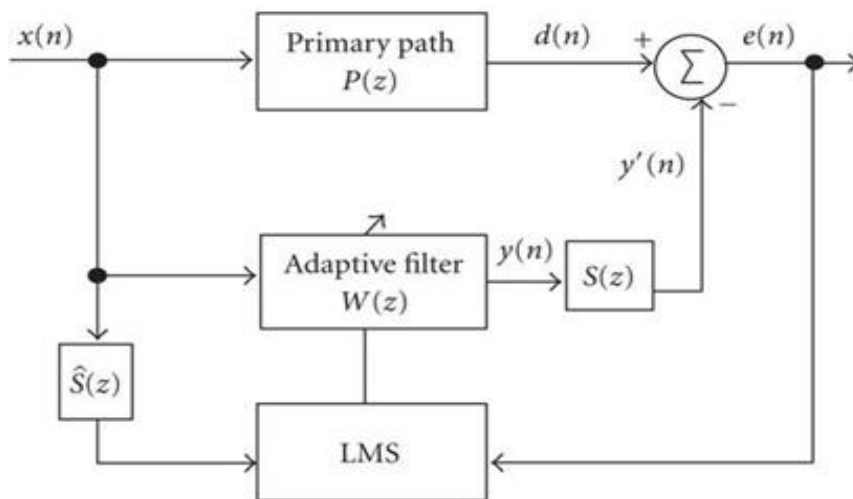

Fig. 1: Narrowband feedforward ANC system

Fig. 2: FxLMS Algorithm-based ANC system

This section of the paper discusses the evolution of linear ANC approaches over the last decade and their possible applications. There are two fundamental methods to ANC systems: Feed forward and feedback methods and a hybrid method have been developed by combining these two approaches. Nakrani and Patel (2012) examined these two techniques for the wide-band and narrow-band noise scenarios while maintaining the filter order and step size constant. It was determined that the feedback technique performed better in the presence of narrow-band noise, but the feed-forward strategy performed well in the presence of wide-band noise.

Das and Panda (2004) suggested a feedback ANC strategy based on the Functional Link Artificial Neural Networks (FLANN) and the Filtered-S Least Mean Square (FSLMS) algorithm. While this approach can minimize certain nonlinear noise, the overall noise cancellation efficiency for random noise signals is low. To address this issue, Luo *et al*. (2017) offered an improved feedback approach based on the wavelet packet FxLMS technique that broke down broadband noise into many band-limited components that could be controlled independently, allowing for fine control over chaotic noise suppression and improved random noise mitigation.

While the feedback technique is substantially less expensive to construct, it does have certain limitations, including comparable stability concerns to IIR filters and the 'waterbed effect,' which suggests that it is extremely unlikely to suppress noise at all frequencies simultaneously. Wu *et al*. (2018) proposed a method for controlling the noise amplifiers in the feedback loop caused by the waterbed effect by substituting a real symmetric Toeplitz matrix for the scaly leaky factor in the leaky FxLMS technique, which ultimately resulted in the effective adjustment of the noise amplification frequency band. Milani *et al*. (2010) investigated the effectiveness of ANC systems from the standpoint of the maximum possible noise attenuation level (NALmax) for three types of ANC systems: Feed-forward, feedback, and hybrid. It was first assessed for stochastic and generalized sinusoidal noise signals, with the results serving as a guide for selecting the right ANC structure for our purposes.

Lee and Park (2013) developed a technique for minimizing MRI noise by identifying the property of MRI noise with a high Sound Pressure Level (SPL) and proposing an open-loop control method based on the noise ensemble average and extra adaptive control for lowering the residue generated in practice. introduced two new techniques that are enhanced

versions of FxLMS: The Filtered-X Wilcoxon LMS (FxWLMS) and the Filtered-X least mean log square (FxLMLS). They are shown to be effective at canceling abnormal feedback in the presence of outliers.

The convergence rate of FxLMS algorithms is improved by increasing the step size, but the misadjustment is increased. A Variable Step-Size LMS (VSS) method is used to achieve both speedy convergence and low misadjustment (Lee *et al*., 2015). Table 1 summarizes some of the research conducted on acoustic noise reduction with their merits and their limitations for a better understanding of the topic.

Materials and Methods

Among the different adaptive algorithms described for diverse ANC techniques discussed in the last section, the FxLMS approach is by far the most widely used because of its low computer resource requirements and practically high performance. The feedforward adaptive step-size filtered-x Least Mean Square (AS-FxLMS) mechanism is used in this research as the ANC mechanism to realize noise control in MRI systems. Typically, a feedforward control system is used in situations that have access to the consistent and advanced reference signal. The control system's performance is contingent upon the coherence of the reference signal and the undesirable acoustic noise. In both the time and frequency domain, Fig. 3A depicts a narrow-band MRI signal acquired from the MRI machine and a larger sequence of interfering narrow pulses, while Fig. 3B shows the power spectrum of the narrow-band MRI signal with average white noise.

Another critical component of the FxLMS control system is the way the control signal is generated to adjust for faulty sound reproduction. After the controller calculates the control signal, it is replicated using a variety of components such as filters, amplifiers, and speakers, each with its unique system model. This collection of components is referred to together as the secondary path, $S(z)$. The FxLMS method was developed to account for secondary path dynamics. In the following sub-section, we discuss the mathematical representation of the FxLMS algorithm and the proposed approach elaborately to better understand the working methodology.

Proposed Adaptive Step-Size FxLMS Algorithm (ASFxLMS)

In the FxLMS technique, a balance is reached between the convergence speed, Mean-Square Error (MSE) and the filter's capacity to track signals as their properties vary when the step-size μ is chosen. Initially, the

adaptive filter W has a non-optimal filter coefficient. As a result, the system uses a large step size to quickly change the weights toward the desired output. As the filter reaches the desired steady-state value, the algorithm must reduce the step-size μ to reduce the excess MSE at the error microphone. The practical challenge, on the other hand, is to develop a set of criteria for altering the step-size *μ* so that the adaptive filter creates a tiny surplus MSE while maintaining its ability to respond quickly to changes in signal characteristics (Kozacky and Ogunfunmi, 2014).

Equation 1 can be used for updating the filter coefficients as follows:

$$w_{n+1}(k) = w_n(k) + \mu_n(k)x'(n-k) \tag{1}$$

The adaptive step size is given by $\mu_n(k)$ varied separately for each coefficient '*w*'. The frequency where the gradient estimate switches sign is proportional to the criterion for changing the step size as in Eq. 2:

$$\nabla^2 e^2(n) = -2e(n)x(n-k) \tag{2}$$

It is thus considered based on the assumption that *e(n)x(n-k)* changes sign often, upon which the coefficient $w_n(k)$ reaches its optimum value where the gradient is zero and vice versa. Hence, the step-size $\mu_n(k)$ can vary between successive values as in Eq. 3:

$$\mu_{min} < \mu_n(k) <_{max} \tag{3}$$

When the operation is in a steady state, a larger step size is used to achieve rapid convergence in the adaptive and tracking phases; when the steady-state error is minor, a smaller step size is used.

As some approximation is needed to control step size in variable ANC systems, an effective approach would be to use the adaptive error signal in the process to establish a relation between the error signal and the step size to capture the non-linearity in adjusting the step size. Thus, we can summarize the operational principle as follows: The error is significant during the initial iteration stage to accelerate convergence; when the error approaches zero, a small step is used to produce a reduced steady error. The objective of the ASF LMS approach is to construct a non-linear relationship between both the step size and the error signal for step adjustment.

The proposed approach uses a single-channel feed-forward filtered-x ANC system, where *e(n)* decreases to approach zero gradually while converging, thus, when

e(n) = 0, μ becomes 0. While the convergence speed is faster with higher μ, it can also result in oscillations, whereas, smaller μ can improve the convergence accuracy and reduce the steady-state noise but at a reduced convergence rate. This can be overcome by introducing the arc-tangent function to the above approach, where an inverse tangent value tan^{-1} of the error signal e(n) is given by *atan(e(n))*. The convergence speed increases with the step-size increase with the increase of α, β, and γ in the error signal. The arc-tangent function-based adaptive step size is represented as presented by (Gomathi *et al*., 2016):

$$\mu(n) = a\tan(e(n)) \tag{4}$$

Introducing α, β and γ parameters to account for precise variation, Eq. (5) can be rewritten as:

$$\mu'(n) = \beta a \tan(e(n))^{\gamma} \tag{5}$$

Thus, the proposed ASF LMS algorithm can be written as:

$$w(n+1) = w(n) + \mu'(n)e(n)x'(n) \tag{6}$$

using the arc-tangent function to improve the convergence speed of the error signal.

Experimental Setup

Figure 4 depicts the experimental fMRI testbed. As previously stated, MRI noise can be as loud as 130 dB SPL. To mask the noise, the control speaker must produce that volume of sound. Due to the surrounding magnetic field, we are unable to utilize standard metallic speakers. Therefore, we utilized a non-magnetic speaker array that vibrates employing an MRI magnetic field. A microphone is placed outside of a noise-attenuated channel to specifically record the noises of MRI equipment in operation. The signals produced by the microphones are utilized to minimize the noise output of MRI equipment. For an error microphone, we have used a MEMS microphone composed of polysilicon and fabricated utilizing semiconductor manufacturing procedures, resulting in a durable microphone with a large degree of reproducibility and stable acoustics. To limit the effect of the magnetic field, the MEMS microphones were placed at various distances (given in cms) from the bore and the audio signal from the mic is sampled. The sampling rate is 48 kHz, which is sufficient to cover the microphone's frequency range.
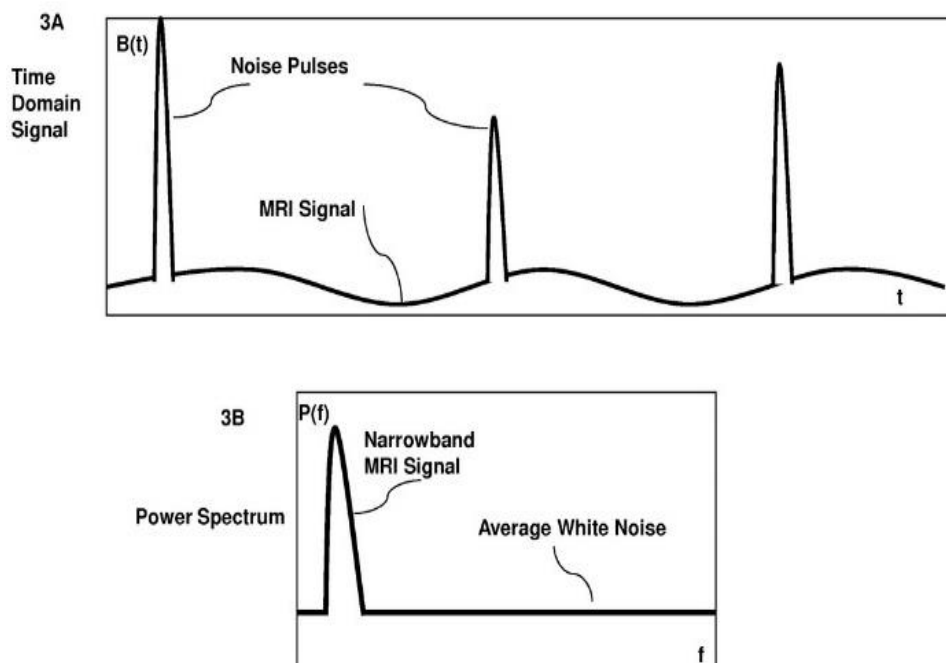
Fig. 3A: Narrowband MRI signal with noise pulses; 3B. Power spectrum of narrowband MRI signal
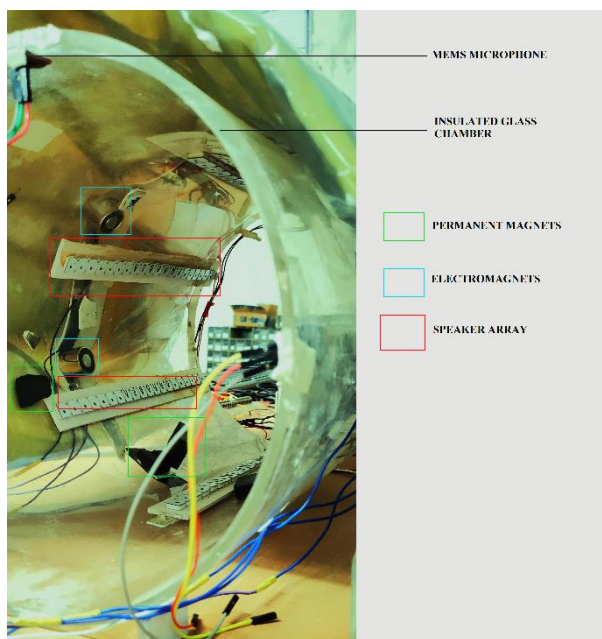
Fig. 4: fMRI test platform in an insulated glass chamber with MEMS microphones, non-magnetic speakers, and electromagnets

Results and Discussion

Simulation Results

For the experimental approach, real-time ANC hardware is not used but is simulated through the code implementation on MATLAB Simulink 2021b. We started designing the desired ANC set up in a simulated environment using MATLAB Simulink prototype design. Thus, we can enhance the model's accuracy or adapt to the experimental setting from the simulated one based on the results. Additionally, we can iterate by modifying our simulated environment as we gain a better understanding of the real-world implementation challenges. This flexibility in the design approach made us choose the Simulink-based environment for the evaluation of our results.

The MRI noise signal for this study was acquired from a GE 3-Tesla whole-body MRI scanner equipped with a diffusion-weighted imaging sequence with the noise measurement focused on the scanner bore isocenter, which is adjacent to the patient's ears and mouth causing the most discomfort during examinations. This pre-recorded noise signal is provided as the input to the Simulink model for processing. For the simulation, the sampling frequency considered is 6 kHz with an adaptive filter length of 32 bits. For computing error signal α, β, and γ for determining the threshold parameters were taken to be 0.05, 0.025, and 0.01, respectively.

The Simulink model design is shown in Fig. 5. We developed an FxLMS ANC system, complete with an ANC controller and variable step-size blocks. As we can design the secondary path later, we suppose that we already have an estimation of the secondary path. We simulate the error microphone signal as the summation of the noise source's primary acoustic path and ANC output's secondary acoustic path filters. We design the "LMS

Update" block in such a way that the signal collected by the error mic is as small as possible. In a Filtered-X model, the LMS update is fed the noise source after it has been filtered by the secondary path estimate. There is a one-sample delay between the generation of the new filter parameters and their usage by the LMS filter to prevent an algebraic loop.

This model has been designed to work in real-time in line with the MRI noise signal fed to it. The noise signal file is converted into data samples and analyzed by the FxLMS block to filter out the noise amplitudes and reduce the error values. The adaptive step process is used to dynamically vary the step-size μ and fed it back to the LMS update block along with the error signal to make corrections to the model. This helps in attaining faster convergence of the model in real-time reducing the noise signal amplitude and the error. The model attains the peak performance where the error and noise levels are normalized in a short time, making it more suitable for experimental scenarios where the noise signal captured by microphones can be fed to the model and the resulting filtered noise can be provided over the speakers in the examination room.

The evaluated simulation results achieved for a 30-sec segment of the pre-recorded MRI noise file are presented in Fig. 6-10. Figure 6 and 7 represent the original noise signal and the filter noise signal with reduced amplitude peaks. From Fig. 8, it can be shown how the adaptive step-size algorithm works in conjunction with the FxLMS algorithm to maintain the step-size to an optimal value to achieve faster convergence while keeping up with the convergence accuracy. Figure 9 shows the error signal

convergence over a 30 sec sample period and it is inferred that the error value is normalized after the initial fluctuations to offer better convergence accuracy. Figure 10 shows the noise signal convergence graph that has a substantial convergence rate in filtering out the MRI noise to about 21 decibels at the end of the sample period, better than other research works discussed in this study.

Experimental Results

For the experimental setup to test the effectiveness of the FxLMS approach on a real-time MRI noise signal, we designed a cylindrical contraption acting as the fMRI test platform that imitates the fMRI bore. For this fMRI test platform, experimental findings from applying the FxLMS with single-tone noises from the MRI machine are shown.

The glass chamber is surrounded by glass wool for insulation. Inside the glass chamber, an array of permanent magnets which produces 0.5 Tesla are placed and its effect on the process of noise reduction is analyzed. Another array of dynamic magnets is attached to the outer surface of the glass chamber Four electromagnets are attached and energized separately. A real-time MRI noise signal from the GE 3T MRI machine is provided as input through the three primary speakers. The acoustic noise is captured by the MEMS microphone that provides the reference signal to the Simulink model where the FxLMS algorithm is used to filter out the unwanted noise using an adaptive step-size approach where the noise gets attenuated until the error signal captured from the error microphone placed at the other end of the glass chamber falls below a threshold level.
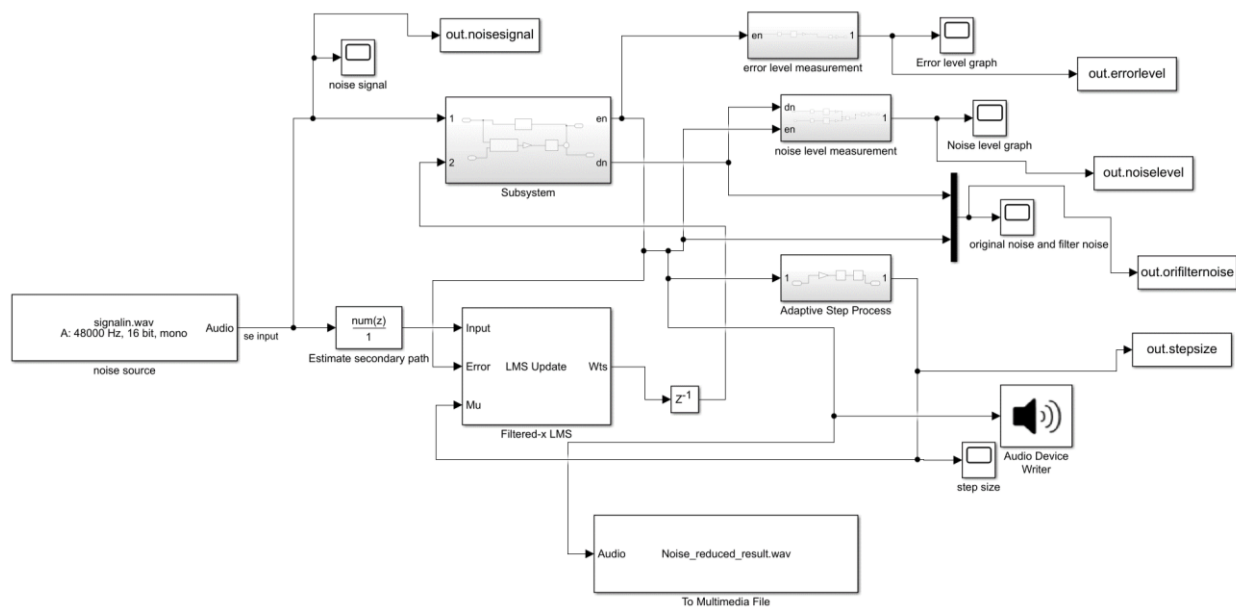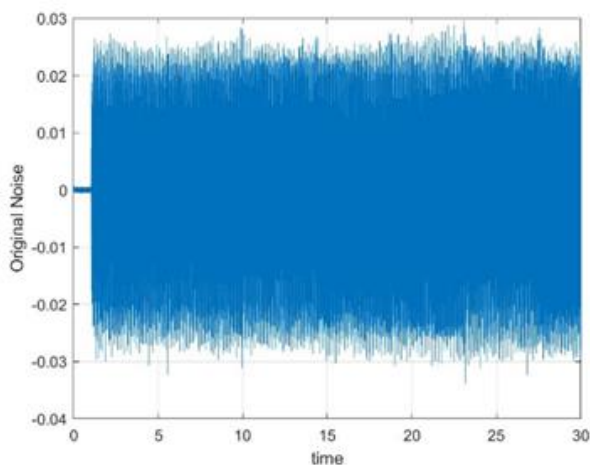

Fig. 5: ASFxLMS Simulink model design
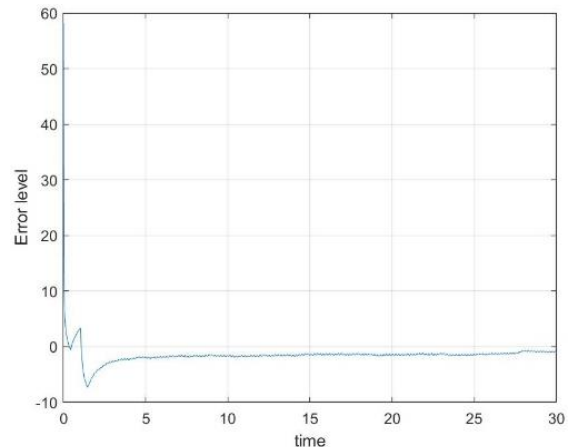
Fig. 6: Original MRI noise signal
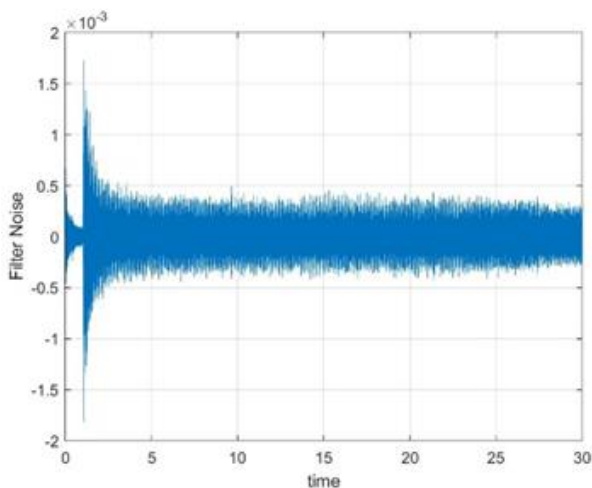
Fig. 7: Filtered noise signal

Fig. 8. Step-size variation over time

Fig. 9: Error signal convergence
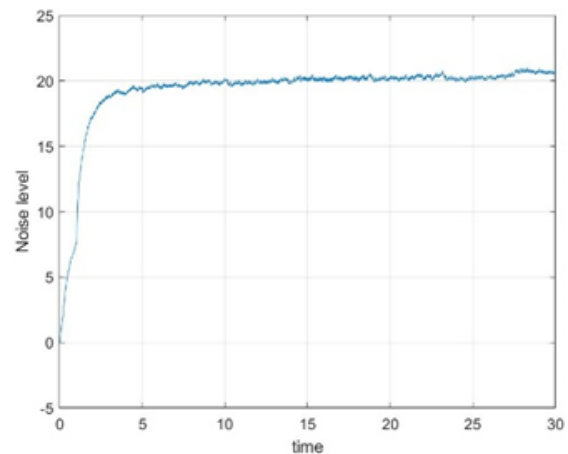
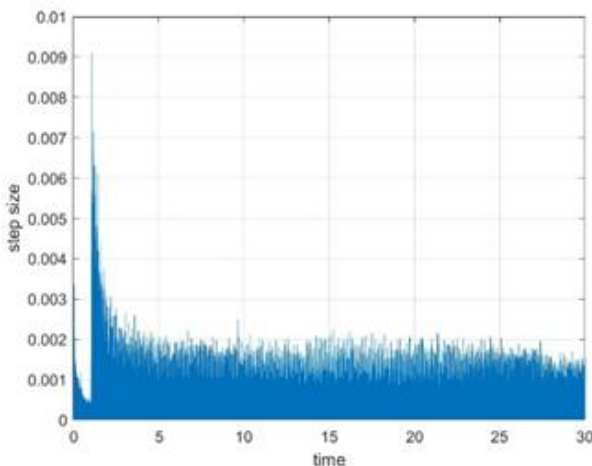**Fig. 10:** Noise level convergence

Table 2 shows the sound levels in dB for both ANC ON and OFF with varying horizontal and combinations of energization of the electromagnets. Electromagnet 1 is energized first and readings are taken. Then Electromagnet 1 and Electromagnet 2 are energized and the effect is studied. Electromagnets 1,2 and 3 are energized and the effect is analyzed. Finally, all four electromagnets are energized which produces 424 Gauss and the effect of this magnetic field is studied. It is found that the presence of a magnetic field does not affect the process of noise reduction. Hence an overall of 25 dB is obtained. The line plots for analysing the ANC for varying positions of the reference microphone from the speakers at different levels of electromagnets are studied in Fig. 11-14. It can be inferred from the figures that the acoustic noise is reduced by a few decibels to about 25 decibels with ANC ON depending on the positioning of the reference microphone. It was also found that there was not any discernible difference in the noise levels with electromagnetic coils energized in any particular sequence, which implies that they have no impact on the acoustic noise in our experimental fMRI testbed as does the

MEMS microphone positioning. We can also deduce from the experiment that as the distance of the reference microphone from the MRI noise source is increased in equal steps, the acoustic noise increases with ANC OFF which can be visualized from the upward trajectory of the acoustic noise levels with the increased vertical distance of the microphone from the reference point. However, with ANC ON, it can be seen that the MRI noise levels are reduced further as the vertical distance of the microphone from the reference point is increased. This produces a considerable noise attenuation performance with ANC ON.

Table 1: Comparison of related literature in acoustic noise reduction

Author(s) (Year)	Technique used	Research Merits	Limitations
Narasimhan *et al.* (2010)	Variable step-size Griffiths' LMS (VGLMS) algorithm is used.	The convergence rate of the feedforward and feedback ANC is faster.	Largely insensitive to measurement noise power.
Jiao *et al.* (2013)	A novel gradient adaptive step size LMS adaptive filter which utilizes two adaptive filters to estimate gradients accurately is used.	Achieves good adaptation and performance. ranges of 10-30 MHz	Suppress frequencies in the bandwidth
Huang *et al.* (2013)	Variable step-size filtered-x LMS (VSS-FXLMS) the algorithm is proposed for a typical narrowband active noise control system.	Better convergence rate is achieved in nonstationary situations.	More computations are required for better efficiency.
Zhou *et al.* (2015)	Normalized frequency-domain block FxLMS (NFB-FxLMS) technique for active vehicle interior noise control.	Has good performance for $S\alpha S$ impulsive noise attenuation. Also, does not require parameter selection and complex gradient computation.	Suffer from signal-dependent noise and low signal-to-noise ratio.
Gomathi *et al.* (2016)	FxLMS algorithm with variable step size to improve the convergence of ANC system has been proposed.	Convergence speed and noise reduction of the variable step algorithm is superior.	On an average, only 13 dB noise reduction is achieved.
Lee *et al.* (2017)	Use a domain transform algorithm, which is time to frequency based on discrete Fourier series, is developed with the same level of computational complexity.	Overall, 35-dB noise reduction in on the 80-1600 Hz range.	It has a fundamental frequency with its higher harmonics.
Zhang *et al.* (2019)	Normalized frequency-domain block FxLMS (NFB-FxLMS) algorithm is proposed for the active vehicle interior noise control.	Faster convergence rate and lower steady-state error in the entire frequency band.	Filter length should be sufficient.
Meng and Chen (2020)	An enhanced GMACFxLMS algorithm (EGMACFxLMS) with amplitude constraint of error signal and input signal is used.	Achieve faster convergence rate and better noise reduction performance.	High impulse noise input is needed to get better noise reduction.

Table 2: Acoustic noise measurement in decibels with ANC ON and OFF concerning the positioning of the microphone and energization of the electromagnets

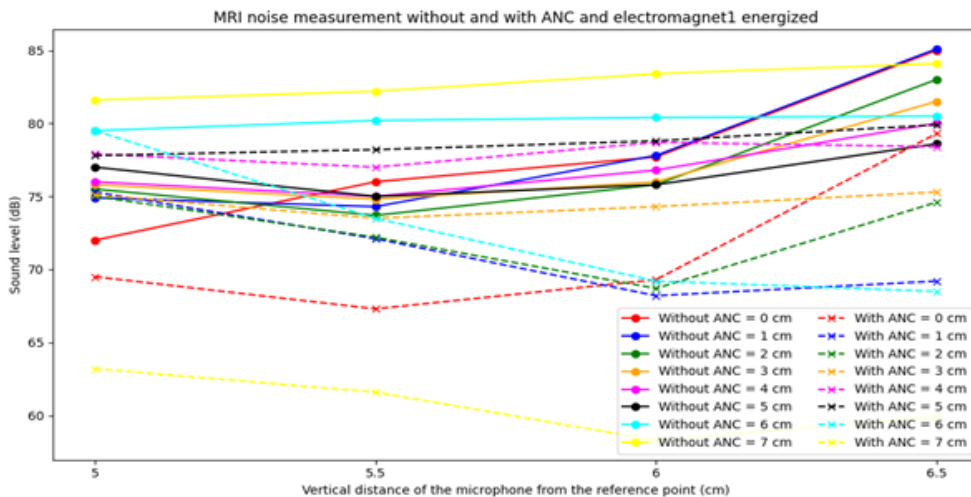| Horizontal length of the microphone from the reference point (cm)	Vertical length of the microphone from the reference point (cm)	Electromagnet 1 energized (101 G) Sound level when ANC is OFF (dB)	Sound level when ANC is ON (dB)	Electromagnet 1 and 2 energized (202 G) Sound level when ANC is OFF (dB)	Sound level when ANC is ON (dB)	Electromagnet 1,2,3, energized (312 G) Sound level when ANC is OFF (dB)	is ON (dB)	Electromagnet 1,2,3, 4 energized (424 G) is OFF (dB)	is ON (dB)
0	5.0	72.0	69.5	70.4	65.5	71.0	67.5	72.0	68.5
	5.5	76.0	67.3	74.0	65.3	76.0	67.3	75.0	67.3
	6.0	77.7	69.3	77.9	69.7	77.7	69.3	75.7	69.3
	6.5	85.0	79.3	85.2	79.6	85.1	78.7	85.4	78.1
1	5.0	74.9	75.3	74.9	75.2	74.7	72.9	74.9	75.2
	5.5	74.3	72.1	74.9	72.6	75.5	73.4	74.9	72.6
	6.0	77.8	68.2	77.5	68.9	77.5	68.8	77.5	68.9
	6.5	85.1	69.2	85.7	67.5	86.3	69.8	85.7	67.5
2	5.0	75.5	75.5	76.8	75.3	76.4	75.6	76.8	75.3
	5.5	73.7	72.2	74.0	72.5	74.3	72.8	74.0	72.5
	6.0	75.8	68.7	76.1	69.0	76.4	69.3	76.1	69.0
	6.5	83.0	74.6	83.3	74.9	83.6	75.2	83.3	74.9
3	5.0	75.8	75.1	76.1	75.4	76.4	75.7	76.1	75.4
	5.5	74.8	73.5	75.1	73.8	75.4	74.1	75.1	73.8
	6.0	76.0	74.3	76.3	74.6	76.6	74.9	76.3	74.6
	6.5	81.5	75.3	81.8	75.6	82.1	75.9	81.8	75.6
4	5.0	76.0	77.9	76.3	78.2	76.6	78.5	76.3	78.2
	5.5	75.0	77.0	75.3	77.3	75.6	77.6	75.3	77.3
	6.0	76.8	78.7	77.1	79.0	77.4	79.3	77.1	79.0
	6.5	80.0	78.4	80.3	78.7	80.6	79.0	80.3	78.7
5	5.0	77.0	77.8	77.3	78.1	77.6	78.4	77.3	78.1
	5.5	75.0	78.2	75.3	78.5	75.6	78.8	75.3	78.5
	6.0	75.8	78.8	76.1	79.1	76.4	79.4	76.1	79.1
	6.5	78.6	79.9	78.9	80.2	79.2	80.5	78.9	80.2
6	5.0	79.5	79.5	79.8	79.8	80.1	80.1	79.8	79.8
	5.5	80.2	73.5	80.5	73.8	80.8	74.1	80.5	73.8
	6.0	80.4	69.2	80.7	69.5	81.0	69.8	80.7	69.5
	6.5	80.5	68.5	80.8	68.8	81.1	69.1	80.8	68.8
7	5.0	81.6	63.2	81.9	63.5	82.2	63.8	81.9	63.5
	5.5	82.2	61.6	82.5	61.9	82.8	62.2	82.5	61.9
	6.0	83.4	58.3	83.7	58.6	84.0	58.9	83.7	58.6
	6.5	84.1	59.9	84.4	60.2	84.7	60.5	84.4	60.2

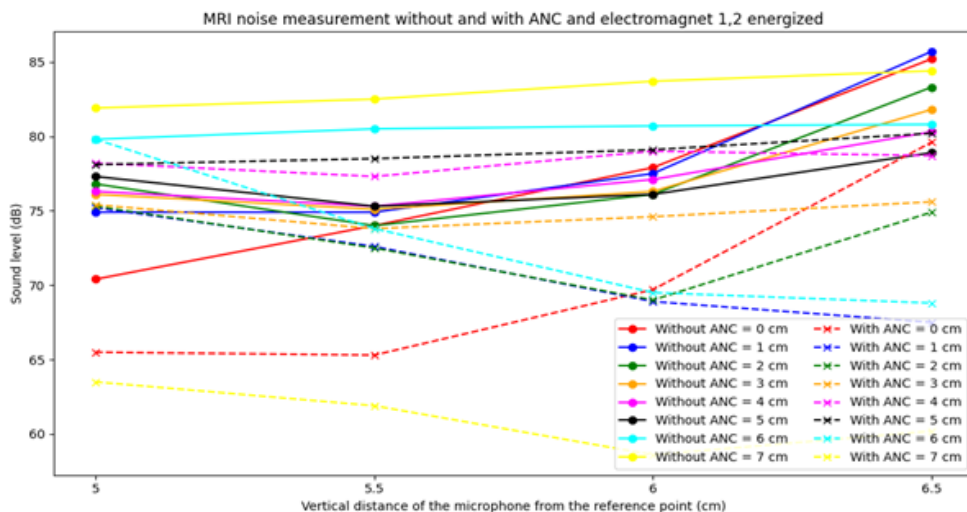**Fig. 11:** MRI noise measurement without and with ANC and electromagnet 1 energized

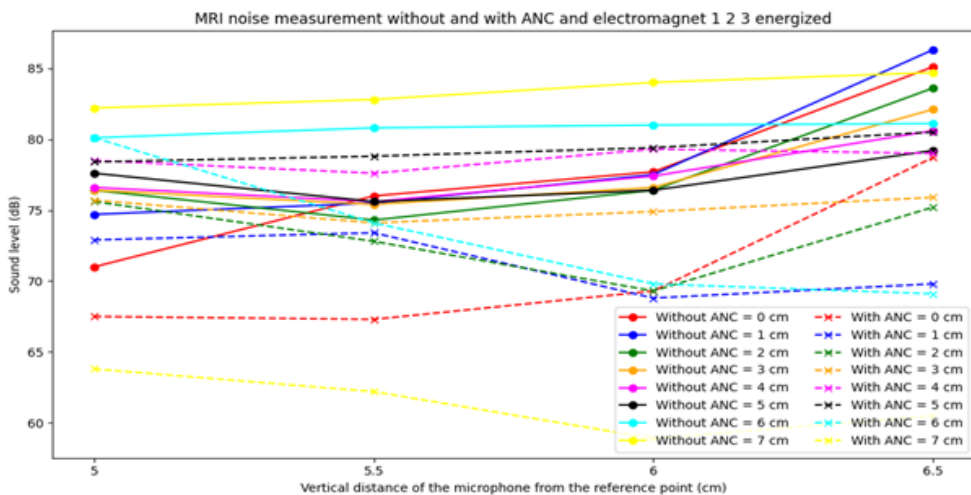**Fig. 12:** MRI noise measurement without and with ANC and electromagnet 1, 2 energized

Fig. 13: MRI noise measurement without and with ANC and electromagnet 1, 2, 3 energized
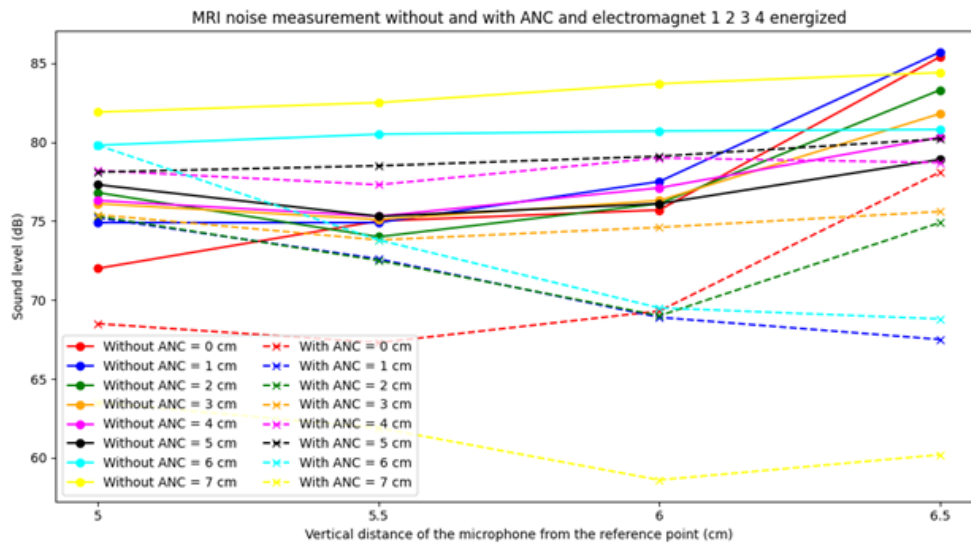
Fig. 14: MRI noise measurement without and with ANC and electromagnet 1, 2, 3, 4 energized

Conclusion

To conclude the work, the simulation results provide ample evidence to show that our approach to acoustic noise reduction based on ASF´s LMS algorithm provides a substantial reduction in acoustic noise with a faster convergence rate of noise and error signals without compromising on the convergency time and accuracy. As the MRI noise was reduced significantly at a shorter time, this approach was also presented experimentally with the fMRI testbed hardware arrangement with electromagnets, MEMS microphone, and speaker array to practically examine the performance of the proposed algorithm during MRI scans. These experimental results were consistent with the simulation results, demonstrating that the ASF´s LMS approach has an extremely high convergence rate and a maximum of 25 dB acoustic noise reduction on average. Motivated by the success of this approach, we plan to extend the MRI acoustic noise reduction research to include non-linear ANC procedures and compare their performance with existing research.

Acknowledgment

Funding Information

Author's Contributions

I. Juvanna: Collected the data, devised the Methodology, performed the analysis and original draft preparation.

Uppu Ramachandraiah: Contributed for Conceptualization, Supervision and performed the data analysis.

G. Muthukumaran: Performed investigation, validation, data analysis and purchase of components.

Kawin Subramaniyam: Data visualization and Data analysis.

G. Nethra: Review, edited and data analysis.

Ethics

This article is substantially original in its approach to the topic of research and the corresponding author confirms that all of the other authors have read and approved the manuscript and that no ethical issues are involved.

References

Akhtar, M. T. & Mitsuhashi, W. (2011). Variable step-size-based method for acoustic feedback modeling and neutralization in active noise control systems. *Applied Acoustics*, 72(5), 297–304. https://doi.org/10.1016/j.apacoust.2010.12.003

Akhtar, M. T., Abe, M. & Kawamata, M. (2007). On active noise control systems with online acoustic feedback path modeling. *IEEE Transactions on Audio, Speech and Language Processing*, 15(2), 593–600. https://doi.org/10.1109/TASL.2006.876749

Chambers, J., Bullock, D., Kahana, Y., Kots, A., & Palmer, A. (2007). Developments in active noise control sound systems for magnetic resonance imaging. *Applied Acoustics*, 68(3), 281–295. https://doi.org/10.1016/j.apacoust.2005.10.008

Chang, C. Y., Kuo, S. M., & Huang, C. W. (2018). Secondary path modeling for narrowband active noise control systems. *Applied Acoustics*, 131 (October 2017), 154–164. https://doi.org/10.1016/j.apacoust.2017.10.026

Das, D. P., & Panda, G. (2004). Active mitigation of nonlinear noise processes using a novel filtered-s LMS algorithm. *IEEE Transactions on Speech and Audio Processing*, 12(3), 313–322. https://doi.org/10.1109/TSA.2003.822741

Facciolo, G., Pierazzo, N., & Morel, J. M. (2017). Conservative scale recomposition for multiscale denoising (the devil is in the high-frequency detail). *SIAM Journal on Imaging Sciences*, 10(3), 1603-1626. https://doi.org/10.1137/17M1111826

Gomathi, K., Saravanan, V., & Santhiya Kumari, N. (2016). Variable step-size for improving convergence of FxLMS algorithm. *Procedia Technology*, 25(Raerest), 420–426. https://doi.org/10.1016/j.protcy.2016.08.127

Haseeb, A., Tufail, M., Ahmed, S., & Ahmed, W. (2018). A robust approach for online feedback path modeling in single-channel narrow-band active noise control systems using two distinct variable step size methods. *Applied Acoustics*, 133(October 2017), 133–143. https://doi.org/10.1016/j.apacoust.2017.12.015

Huang, B., Xiao, Y., Sun, J., & Wei, G. (2013). A variable step-size FXLMS algorithm for narrowband active noise control. *IEEE Transactions on Audio, Speech and Language Processing*, 21(2), 301–312. https://doi.org/10.1109/TASL.2012.2223673

Jiao, Y., Cheung, R. Y. P., Chow, W. W. Y., & Mok, M. P. C. (2013). A novel gradient adaptive step size LMS algorithm with dual adaptive filters. *Proceedings of the Annual International Conference of the IEEE Engineering in Medicine and Biology Society*, EMBS, 4803–4806. https://doi.org/10.1109/EMBC.2013.6610622

Khan, I., Muthusamy, D., Ahmad, W., Sällberg, B., Nilsson, K., Zackrisson, J., Gustavsson, I., & Håkansson, L. (2012). Performing active noise control and acoustic experiments remotely. *International Journal of Online Engineering*, 8(SPECIAL ISSUE 2), 65–74. https://doi.org/10.3991/ijoe.v8iS4.2304

Kozacky, W. J., & Ogunfunmi, T. (2014). A cascaded IIR-FIR adaptive ANC system with output power constraints. *Signal Processing*, 94(1), 456–464. https://doi.org/10.1016/j.sigpro.2013.06.036

Kuo, S. M., Kong, X., & Gan, W. S. (2003). Applications of adaptive feedback active noise control system. *IEEE Transactions on Control Systems Technology*, 11(2), 216–220. https://doi.org/10.1109/TCST.2003.809252

Kuo, S. M., Mitra, S., & Gan, W. S. (2006). Active noise control system for headphone applications. *IEEE Transactions on Control Systems Technology*, 14(2), 331–335. https://doi.org/10.1109/TCST.2005.863667

Lee, H. S., Kim, S. E., Lee, J. W., & Song, W. J. (2015). A variable step-Size diffusion LMS algorithm for distributed estimation. *IEEE Transactions on Signal Processing*, 63(7), 1808–1820. https://doi.org/10.1109/TSP.2015.2401533

Lee, N., & Park, Y. (2013). A method of using open-loop and adaptive control for reducing MRI noise. *International Conference on Control, Automation, and Systems*, Iccas, 1781–1783. https://doi.org/10.1109/ICCAS.2013.6704227

Lee, N., Park, Y., & Lee, G. W. (2017). Frequency-domain active noise control for magnetic resonance imaging acoustic noise. *Applied Acoustics*, 118, 30–38. https://doi.org/10.1016/j.apacoust.2016.11.003

Lin, J. H., Li, P. C., Tang, S. T., Liu, P. T., & Young, S. T. (2005). Industrial wideband noise reduction for hearing aids using a headset with adaptive-feedback active noise cancellation. *Medical and Biological Engineering and Computing*, 43(6), 739–745. https://doi.org/10.1007/BF02430951

Lu, L., Yin, K. L., de Lamare, R. C., Zheng, Z., Yu, Y., Yang, X., & Chen, B. (2021). A survey on active noise control in the past decade-Part I: Linear systems. *Signal Processing*, 183. https://doi.org/10.1016/j.sigpro.2021.108039

Luo, L., Sun, J., & Huang, B. (2017). A novel feedback active noise control for broadband chaotic noise and random noise. *Applied Acoustics*, 116, 229–237. https://doi.org/10.1016/j.apacoust.2016.09.029

Mazur, K., Wrona, S., & Pawelczyk, M. (2018). Design and implementation of multichannel global active structural acoustic control for a device casing. *Mechanical Systems and Signal Processing*, 98, 877–889. https://doi.org/10.1016/j.ymssp.2017.05.025

McJury, M. J. (2021). Acoustic noise and magnetic resonance imaging: A narrative/descriptive review. *Journal of Magnetic Resonance Imaging*. https://doi.org/10.1002/jmri.27525

Meng, H., & Chen, S. (2020). A modified adaptive weight-constrained FxLMS algorithm for feedforward active noise control systems. *Applied Acoustics*, 164,107227. https://doi.org/10.1016/j.apacoust.2020.107227

Milani, A. A., Kannan, G., & Panahi, I. M. S. (2010). On maximum achievable noise reduction in ANC systems. *2010 IEEE International Conference on Acoustics, Speech and Signal Processing*, 349–352. https://doi.org/10.1109/ICASSP.2010.5495853

Nakrani, N., & Patel, N. (2012). Feed-forward and feedback active noise control system using fxlms algorithm for narrowband and broadband noise. *Proceedings - International Conference on Communication Systems and Network Technologies*, CSNT 2012, 1, 577–580. https://doi.org/10.1109/CSNT.2012.130

Narasimhan, S. V., Veena, S., & Lokesha, H. (2010). Variable step-size Griffiths' algorithm for improved performance of feedforward/feedback active noise control. *Signal, Image and Video Processing*, 4(3), 309–317. https://doi.org/10.1007/s11760-009-0120-9

Panda, G., & Puhan, N. B. (2016). A robust adaptive hybrid feedback cancellation scheme for hearing aids in the presence of outliers. *Applied Acoustics*, *102*, 146-155. https://doi.org/10.1016/j.apacoust.2015.09.007

Price, D. L., De Wilde, J. P., Papadaki, A. M., Curran, J. S., & Kitney, R. I. (2001). Investigation of acoustic noise on 15 MRI scanners from 0.2 T to 3 T. *Journal of Magnetic Resonance Imaging*, 13(2), 288–293. https://doi.org/10.1002/1522-2586 (200102)13:2<288::AID-JMRI1041>3.0.CO;2-P

Roozen, N. B., Koevoets, A. H., & den Hamer, A. J. (2008). Active vibration control of gradient coils to reduce acoustic noise of MRI systems. *IEEE/ASME Transactions on Mechatronics*, 13(3), 325–334. https://doi.org/10.1109/TMECH.2008.924111

Rudd, B. W., Lim, T. C., Li, M., & Lee, J. H. (2012). In situ active noise cancellation applied to magnetic resonance imaging. *Journal of Vibration and Acoustics, Transactions of the ASME*, 134(1), 1–7. https://doi.org/10.1115/1.4005008

Siddiqui, Z., Singh, P., Kushwaha, S., & Srivastava, R. (2017). MRI and fear of confined space: A cause-and-effect relationship. *International Journal of Contemporary Medicine Surgery and Radiology*, 2(1), 19–24.

Takkar, M. S., Kumar Sharma, M., & Pal, R. (2018). A review on the evolution of acoustic noise reduction in MRI. *2017 Recent Developments in Control, Automation and Power Engineering*, *RDCAPE* 2017, 3, 235–240. https://doi.org/10.1109/RDCAPE.2017.8358273

Wu, L., Qiu, X., & Guo, Y. (2014). A simplified adaptive feedback active noise control system. *Applied Acoustics*, 81, 40–46. https://doi.org/10.1016/j.apacoust.2014.02.006

Wu, L., Qiu, X., & Guo, Y. (2018). A generalized leaky FxLMS algorithm for tuning the waterbed effect of feedback active noise control systems. *Mechanical Systems and Signal Processing*, 106, 13–23. https://doi.org/10.1016/j.ymssp.2017.12.021

Zeb, A., Mirza, A., Khan, Q. U., & Sheikh, S. A. (2017). Improving the performance of the FxRLS algorithm for active noise control of impulsive noise. *Applied Acoustics*, 116, 364–374. https://doi.org/10.1016/j.apacoust.2016.10.011

Zhang, S., Wang, Y. S., Guo, H., Yang, C., Wang, X. L., & Liu, N. N. (2019). A normalized frequency-domain block filtered-x LMS algorithm for active vehicle interior noise control. *Mechanical Systems and Signal Processing*, 120(333), 150–165. https://doi.org/10.1016/j.ymssp.2018.10.031

Zhou, Y., Zhang, Q., & Yin, Y. (2015). Active control of impulsive noise with symmetric α-stable distribution based on an improved step-size normalized adaptive algorithm. *Mechanical Systems and Signal Processing*, 56, 320–339. https://doi.org/10.1016/j.ymssp.2014.10.002